Molecular Vision 2020; 26:226-234 <http://www.molvis.org/molvis/v26/226>
Received 19 August 2019 | Accepted 24 March 2020 | Published 26 March 2020

Mutation spectrum of *PAX6* and clinical findings in 95 Chinese patients with aniridia

Bing You, Xiaohui Zhang, Ke Xu, Yue Xie, Hanwen Ye, Yang Li

Beijing Institute of Ophthalmology, Beijing Tongren Eye Center, Beijing Tongren Hospital, Capital Medical University, Beijing Ophthalmology & Visual Sciences Key Lab. Beijing, China

Purpose: Aniridia is a rare congenital panocular disease caused by mutations in *PAX6*. The purposes of this study were to clarify the mutation features of *PAX6* in a cohort of Chinese patients with aniridia and to describe their clinical characteristics.

Methods: We recruited 95 patients from 65 unrelated families clinically diagnosed with aniridia. All patients underwent ophthalmic examinations. Sanger sequencing and multiplex ligation probe amplification of *PAX6* were performed to detect intragenic variants and copy number variations (CNVs).

Results: We identified 58 disease-causing mutations in *PAX6* in 63 families; the detection rate was 96.9%. The 58 mutations included frameshift indels (27.6%), splice site changes (25.9%), nonsense mutations (20.7%), CNVs (19.0%), missense mutations (3.4%), run-on mutations (1.7%), and a synonymous mutation (1.7%). Clinical examinations revealed that 71 patients had complete or almost complete iris loss, 16 patients showed partial iris loss, and six patients had a full iris but with an abnormal structure.

Conclusions: The results confirmed that mutations in *PAX6* are the predominant cause of aniridia, and the majority are loss-of-function mutations that usually result in classical aniridia. In contrast, missense mutations, run-on mutations, and small numbers of splicing mutations mostly lead to atypical aniridia and an intrafamilial phenotypic variability of iris hypoplasia.

Aniridia is a rare congenital panocular disease characterized by a variable degree of hypoplasia of the iris and an incidence rate of between 1:40,000 and 1:96,000 [1-3]. Most patients with aniridia also have nystagmus, foveal hypoplasia, and visual defects. As the disease progresses, 50–90% of patients may develop keratopathy, cataract, and glaucoma in childhood or in the first two decades of life [1]. Aniridia may present as an isolated ocular disorder or as a part of Wilms' tumor, aniridia, genitourinary abnormalities, mental retardation (WAGR) syndrome, and obesity (WAGRO) syndrome [1-3]. Aniridia is an autosomal dominant disorder with high penetrance and variable expression. Approximately two-thirds of aniridia cases have an affected parent, and the remaining one-third of patients are sporadic, usually carrying a de novo gene mutation. Mutations in the paired box 6 (*PAX6*; Gene ID: 5080, OMIM: 607108) gene and its associated regulatory regions are major causes of aniridia [1-3].

The *PAX6* gene, located on chromosome 11p13, encodes a highly conserved transcriptional regulatory protein that is expressed in the developing eye, brain, spinal cord, and pancreas [4,5]. The protein consists of two DNA binding domains—a paired domain (PD) and a homeodomain (HD) separated by a 79-amino acid linker peptide (LNK)—and a proline, serine, and threonine-rich (PST) transcriptional transactivation domain [4,5]. Thus far, more than 400 distinct *PAX6* variants have been reported based on the Human PAX6 Mutation Database) [6]. The majority (about 77%) of the reported intragenic mutations are nonsense, frameshift small insertion or deletion (indel), and splicing mutations that introduce a premature termination codon (PTC) and trigger a nonsense-mediated decay (NMD) process [6]. Missense mutations account for only 11.7% of the intragenic mutations of *PAX6* [6]. Large heterozygous genomic deletions at the 11p13 region that include *PAX6* or its associated regulatory regions have also been frequently reported [6-9]. These loss-of-function nucleotide variants and haploinsufficiency of *PAX6* represent the main mechanism underlying the occurrence of aniridia [6,7].

To date, *PAX6*-related aniridia in Caucasian patients has been extensively described [10-13]. However, similar studies on the *PAX6* mutation spectrum and the clinical features in Chinese patients are limited, especially in large cohorts. In the present study, we screened mutations in *PAX6* in 95 patients drawn from 65 unrelated families who showed different extents of hypoplasia of the iris. We described their phenotypes in detail and used minigene analysis to evaluate

Correspondence to: Yang Li, Beijing Institute of Ophthalmology, Beijing Tongren Hospital, Hougou Lane 17, Chong Nei Street, Beijing, 100730, China; Phone: 8610-58265915; FAX: 8610-65288561 or 65130796; email: yanglibio@aliyun.com

the influence of three single nucleotide variants (SNVs) on the splicing pattern.

METHODS

Participants: This study was performed according to the tenets of the Declaration of Helsinki for research involving human subjects and was approved by the Beijing Tongren Hospital Joint Committee on Clinical Investigation (Beijing, China). This study also adhered to the ARVO statement on human subjects. Informed consent was obtained from all patients after a full explanation of the procedures. We enlisted 95 patients with aniridia from 65 unrelated families, including five previously described families [14,15]. Of these families, 39 probands had a family history showing an autosomal dominant inheritance pattern, while the remaining 26 probands were sporadic. All patients underwent a standard ophthalmological examination consisting of best-corrected visual acuity (BCVA), slip-lamp biomicroscopy, and fundus examination. About half of the patients also underwent optical coherence tomography (OCT) examinations (Heidelberg OCT Spectralis, Heidelberg, Germany, or Ivue-100, Optovue Inc., Fremont, CA). Aniridia-related keratopathy (ARK) severity was graded into 0 to 4 stages according to the 5-point scale detailed described by Lagali et al. [16] (Figure 1).

PCR-based sequencing of the PAX6 gene and bioinformatics analysis: Peripheral blood samples were obtained by venipuncture from all participants and preserved on 4°C before use. The genomic DNA was extracted using a genomic DNA extraction and purification kit (Vigorous, Beijing, China), following the manufacturer's protocol. Whole exons of the *PAX6* gene (including exon 5a) were amplified with 13 pairs of primers, as previously described [15]. PCR assays were carried out using standard reaction mixtures. After an initial denaturation at 95 °C for 5 min, reaction mixes underwent 35 cycles of 95 °C for 30 s, annealing for 30 s, and 72 °C for 30 s followed by 72 °C for 10 min. The sequencing results were compared with a published cDNA sequence for *PAX6* (GenBank NM_000280.4). In silico analysis was performed using Mutation Taster, PolyPhen-2, and SIFT when a missense variant was encountered. For variants that had a suspected splicing effect, we performed in silico analysis using the NetGene2 Server, Human Splice Finder (HSF), and Berkeley Drosophila Genome Project (BDGP). The pathogenicity assessment was based on the guidelines presented by the American College of Medical Genetics and Genomics (ACMG) [17]. Cosegregation analysis was performed when a *PAX6* variant was detected, and other family members were available.

Multiplex ligation-dependent probe amplification: For 14 patients who had no intragenic PAX6 mutation identified, we performed Multiplex ligation-dependent probe amplification (MLPA) to detect genomic rearrangement in the chromosome 11p13 region. The MLPA analyses were carried out using the SALSA MLPA P219-B2 PAX6 probe mix (MRC Holland, Amsterdam, Netherlands) following the manufacturer's protocol. The detailed methods had been previously described [15].

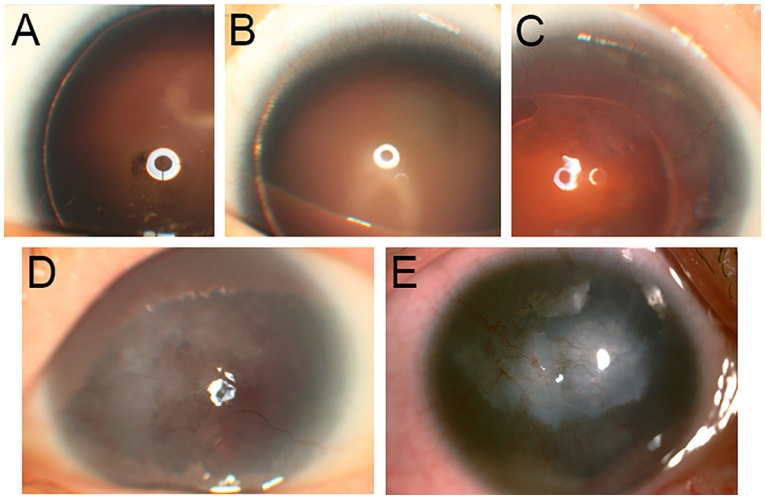

Figure 1. Color anterior segment photographs showing grade 0 to grade 4 ARK, based on the 5-point scale. **A**: Grade 0 aniridia-related keratopathy (ARK): The limbal border is intact (4-year-old boy carrying gross deletion in *PAX6*, *ELP4,* and *DKFZp686K1684*). **B**: Grade 1 ARK: The limbal border is compromised, with vessels and conjunctival tissue invading into no more than 1 mm of the limbus (3-year-old girl carrying mutation p.N9Sfs*17). **C**: Grade 2 ARK: The vessels and conjunctival tissue invade into the mid-peripheral cornea, but at least 2–3 mm of the central cornea is spared (42-year-old woman carrying mutation p.Y90Lfs*2). **D**: Grade 3 ARK: The entire cornea surface is covered by the pannus, but the cornea remains translucent (46-year-old woman carrying mutation p.D23Afs*29). **E**: Grade 4 ARK: The cornea is opaque and vascularized with a thick, irregular pannus (31-year-old man carrying mutation c.141+1G>T).

Minigene assay: We evaluated an effect on splicing of three SNVs (one synonymous and two missense mutations) using minigene assays (Exontrap, MoBiTec GmbH, Goettingen, Germany) and pET01 Exontrap vectors. Human embryonic kidney 293 (HEK-293) cells and human retinal pigmented epithelium-19 (ARPE-19) cells grown under standard conditions were used for transfection. The cells were verified as authentic with short tandem repeat (STR) analysis (detailed methods and results of STR analysis are described in Appendix 1). Primers containing a 5′-BamHI site and a 3′-NotI site were designed to amplify the exon of interest and about 300–700 bp of flanking introns. Amplified genomic DNA from three patients with an SNV and one patient with a canonical splicing mutation c.357+1G>A (as a positive control) was cloned to pET01 Exontrap vectors, according to the manufacturer's instructions. Clones with either the mutant or wild-type allele were detected and selected with Sanger sequencing. The selected cloned minigene plasmids were then transfected into HEK-293 or ARPE-19 cells using Lipofectamine 2000 DNA transfection reagent (Invitrogen, Carlsbad, CA), according to the manufacturer's instructions. Reverse transcription-polymerase chain reaction (RT-PCR) was performed using the FastKing One-Step RT–PCR Kit (Tiangen Biotech). After 48 h, the transfected cells were harvested, and total RNA was extracted with the RNAprep Pure Cell/Bacteria Kit (Tiangen Biotech, Beijing, China). After an initial reverse transcription at 42 °C for 30 min and denaturation at 95 °C for 3 min, reaction mixes underwent 35 cycles of 94 °C for 30 s, 60 °C for 30 s, and 72 °C for 30 s followed by 72 °C for 5 min. The RT-PCR products were analyzed with 2% agarose gel electrophoresis, and each gel-purified DNA band was confirmed with Sanger sequencing.

RESULTS

Genetic findings: We identified 47 distinct intragenic disease-causing mutations in *PAX6* and 11 larger genomic deletions in the chromosome 11p13 region in 63 families, for a detection rate of 96.9%. In two sporadic cases, no disease-causing mutation was detected. The 47 intragenic mutations included 16 frame-shift indel, 15 splicing effect, 12 nonsense, two missense, one run-on, and one synonymous mutation (Appendix 2). The distribution of each intragenic mutation in *PAX6* is shown in Figure 2A. Of the 11 different-length large genomic deletions (from at least 11 kb to 6.2 Mb), seven included a part or all of the *PAX6* gene, three encompassed *PAX6* and *WT1* (Gene ID: 7490, OMIM: 607102), and one involved only the *PAX6* downstream-associated regulatory region (Appendix 2, Figure 2B). The most common mutation was p.X423Lfsext*36, which was identified in four probands with an allele frequency of 6% (4/63). Mutation p.R203X and a gross deletion encompassing *ELP4* (Gene ID: 26610, OMIM: 606985), *PAX6*, and *DKFZp686K1684* were each detected in two probands with an allele frequency of 3% (2/63), while the remaining 55 mutations were each found only in one proband. Of the 58 mutations, 29 mutations were identified for the first time in the present study. These novel mutations were not found in any public databases, such as the Exome Variant Server and 1000 Genomes, and were classified as pathogenic variants based on the ACMG guidelines (Appendix 2).

Two novel missense mutations and one synonymous mutation were predicted by NetGene2 or HSF to affect splicing; therefore, we performed minigene assays to reveal the influences of these mutations on *PAX6* pre-mRNA splicing. The synonymous mutation c.174C>T and the positive control c.357+1G>A introduced a new donor splicing site within exon 6, resulting in a 185 bp and 108 bp shortening of exon 6, respectively (Figure 3A). In contrast, the two missense mutations c.359T>A and c.780T>G did not show any abnormal splicing bands in either HEK-293 or ARPE-19 cells (Figure 3B,C).

Clinical characteristics: In total, 93 patients from 63 unrelated families (24 sporadic and 39 with family history) were found to carry disease-causing mutations in *PAX6*. Cosegregation analyses performed in 56 (89%) unrelated families revealed 21 sporadic probands, each carrying a de novo mutation. (See Appendix 3 for a summary of the clinical findings for the 93 patients.) This cohort of patients included 43 women and girls and 50 men and boys. Their age at last examination ranged from 2 months to 71 years, and their BCVA varied from 0.8 to no light perception (NLP). The patients showed different extents of iris hypoplasia: 67 patients had complete loss of the iris (Figure 4A), four patients had almost complete iris loss (Figure 4B), 16 patients had partial iris loss (Figure 4C), and six patients had a full iris but with abnormal structures (Figure 4D). Overall, 93% of the patients (70/75) whose fundi were examinable with ophthalmoscopy or OCT presented foveal hypoplasia (Figure 4E,F). In addition, 87% of the patients (59/68) whose ARK was evaluated and graded with color anterior segment photography showed stage 1–4 keratopathy (Supplementary Table S2-Appendix 3). We also observed nystagmus (87%), cataract (87%), glaucoma (15%), microcornea (13%), tunica vasculosa lentis (TVL) or persistent pupillary membrane (12%), ectopia lentis (3%), and optic nerve hypoplasia (ONH; 1%) in the patients. Three sporadic patients who presented with non-ocular complications were diagnosed with WAGR (026130 and 026155) and WAGRO (026046) syndromes. We observed intrafamilial phenotype

heterogeneity in five families (026027, 026058, 026059, 026123, and 026151; Figure 5).

Two patients (026071 and 026136) had no mutation in *PAX6*, and both showed partial loss of the iris (Appendix 4).

Genotype–phenotype correlation: All 71 patients with complete or almost complete iris loss carried either gross genomic deletions or frameshift indel, nonsense, or splicing effect mutations. All the splicing effect mutations identified in the 71 patients were predicted to introduce a PTC, except mutation c.357+1G>A (which resulted in an in-frame deletion of PAX6) and mutation c.-128–1G>C. In contrast, six patients with the run-on mutation p.X423Lfsext*36 all presented with a partial loss of the iris, and four patients with two missense mutations displayed full or partial iris loss. Of the five families showing intrafamilial phenotypic variability, two families were detected with missense mutations (p.V120E and p.N260K), two pedigrees had splicing effect mutations (c.-128–1G>C and c.1183+5G>A), and one family had a small frameshift deletion (p.P286Lfs*79). A novel mutation c.-128–1G>C in intron 2 was presumed to result in a skipping of exon 3 (77 bp); this mutation was located in the upstream of the coding region of *PAX6*. Mutation c.1183+5G>A, located in intron 12 and presumed to escape the NMD process (Figure 2A), was predicted to introduce a frameshift at amino acid 396 and add 15 residues to the C-terminal region of the PAX6 protein. Of the 68 patients whose ARK was graded, their ARK severity increased with aging; however, the patients carrying non-NMD mutations seemed to have milder ARK than the patients carrying gross deletions and NMD mutations (Appendix 3).

Five patients from family 026016 carried a gross deletion that encompassed only *ELP4* and *DCDC1* (Gene ID: 341019, OMIM: 608062). All five of these patients had relatively better visual acuity than that observed in either the patients with gross deletions involving *PAX6* or in the patients with NMD mutations. These five patients were also the only ones in this cohort who did not present with foveal hypoplasia.

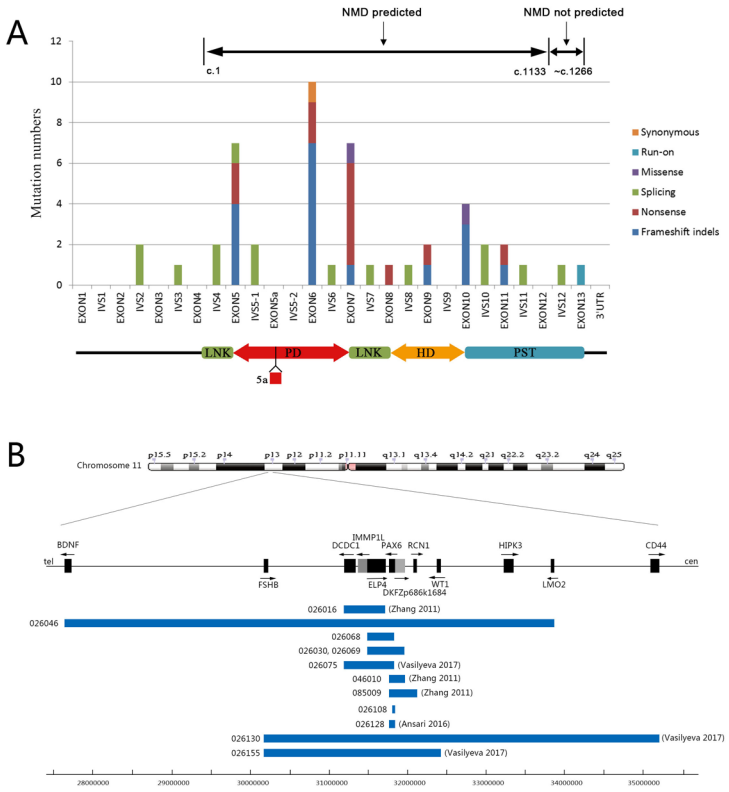

Figure 2. The distribution of 58 distinct mutations in *PAX6* detected in the present study. **A**: The distribution of 47 intragenic mutations on exons and introns of *PAX6* and the corresponding domain of PAX6. LNK, HD, PD, and PST indicate the linker region, homeodomain, paired domain, and proline-threonine-serine-rich domain, respectively. NMD, nonsense-mediated decay; IVS, intron. **B**: Lengths and positions of the 11 gross deletions involving *PAX6* on chromosome 11p13. Cen indicates the centromere, and tel indicates the telomere. Gray and black squares indicate different genes. Genes are shaded in different colors when they are near each other. The arrows indicate the coding direction of each gene, and 026xxx indicates the patient ID.

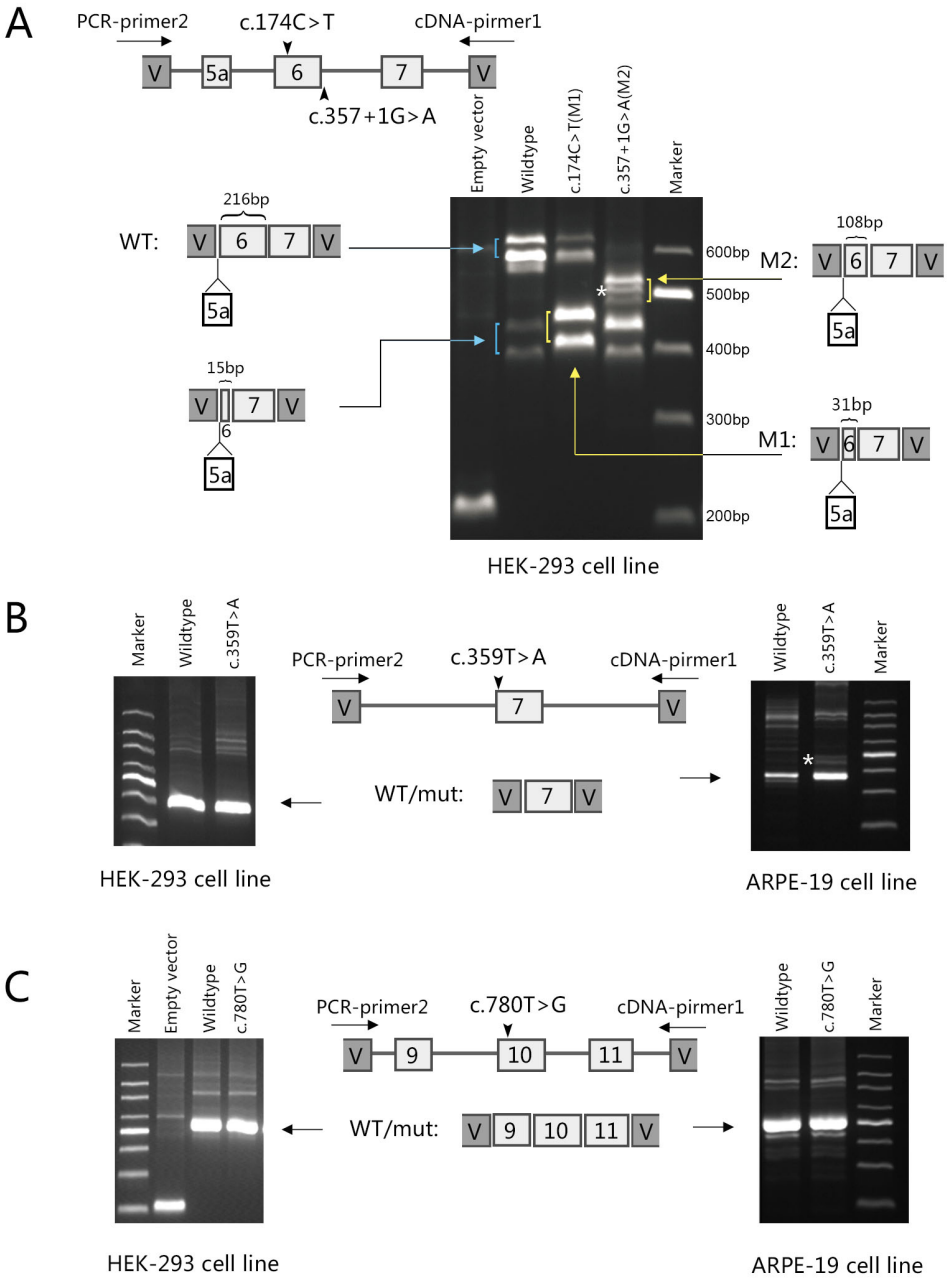

Figure 3. Splicing results of minigene assays for three mutations in *PAX6* in the HEK-293 or ARPE-19 cell lines. The schematics of the minigene constructs are depicted as follows: deep gray squares = vectors, V = vector; light gray squares = *PAX6* exons; thick lines = *PAX6* introns; mutations are marked on the corresponding positions on the exons. PCR-primer2 and cDNA-primer1 were the primers used for reverse transcription-polymerase chain reaction (RT-PCR) and sequencing. The bands labeled "*" represent an artifact of the experimental process. **A**: RT–PCR analysis of minigene splicing for synonymous mutation c.174C>T and positive control c.357+1G>A in a transfected human embryonic kidney 293 (HEK-293) cell line. Exon 5a was alternatively spliced in the wild-type and mutant constructs. The wild type showed two splicing patterns: 629 bp (with exon5a)/587 bp and 428/386 bp, while mutation c.174C>T (M1) presented abnormal splicing bands 444/402 bp that resulted in a 185 bp shortening of exon 6. The positive control c.357+1G>A (M2) also showed abnormal splicing bands 521/479 bp that led to a 108 bp deletion of exon 6. (**B**) and (**C**). RT–PCR analysis of minigene splicing of missense mutations c.359T>A and c.780T>G in transfected HEK-293 and human retinal pigmented epithelium-19 (ARPE-19) cell lines. Wild-type and mutant minigenes showed a normal splicing pattern, and no abnormal splicing bands were observed. WT: wild-type; mut: mutant.

DISCUSSION

In this study, we screened the *PAX6* gene in 95 patients from 65 unrelated families, making this the largest cohort of patients with congenital aniridia examined thus far in the Chinese population. We identified mutations in the *PAX6* gene in 96.9% of the probands with aniridia, which was similar to the previous reports on two recent large cohort studies [11,12]. However, the present detection rate was much higher than the one (55%) previously reported in a Chinese cohort that included 38 probands [18].

The 58 distinct mutations identified in the present study included almost all types of mutation in *PAX6*. Of the 47 intragenic mutations, 19 were detected in the PD (40%), followed by ten mutations in the LNK regions (21%), ten

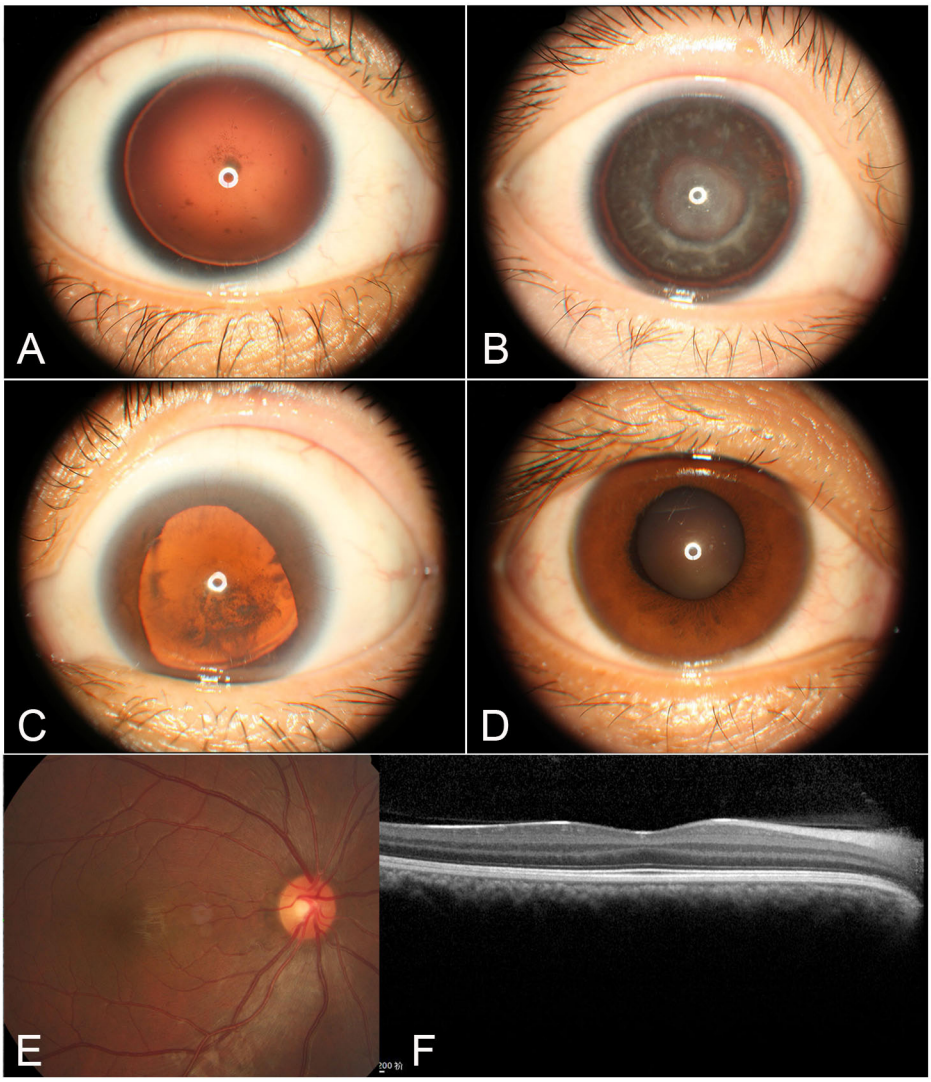

Figure 4. CAS, fundus photographs, and OCT scanning of patients with mutations in *PAX6* showing the different extent of iris defects and foveal hypoplasia. **A**: Color anterior segment (CAS) of Patient 026079 with mutation p.Q47X showing a complete loss of the iris. **B**: CAS photograph of Patient 026049 with mutation c.-52+1G>T presenting a nearly complete loss of the iris. **C**: CAS photographs of Patient 026085 with mutation p.X423Lfsext*36 showing partial loss of the iris. **D**: CAS photograph of Patient 026123-1 with mutation c.1183+5G>A presenting with a full iris but with ectropion uveae. **E** and **F**: Fundus photograph and optical coherence tomography (OCT) scanning of Patient 026123-1 displaying foveal hypoplasia.

mutations in the PST transactivation domain (21%), five mutations in the HD (11%), and three mutations in the 5′ untranslated region (6%). Analysis of the different types of mutations in *PAX6* and their locations can help distinguish potential functional effects of the nature of the mutations. The 16 frameshift indels and 12 nonsense mutations were located between exons 5 and 11, where a PTC can activate the NMD process [7]. The minigene assay results demonstrated that the synonymous mutation c.174C>T also introduced a PTC in exon 6, as previously described [19]. Among the 15 splice mutations, nine were predicted to introduce a PTC that could subsequently activate the NMD process, while the remaining six mutations were relatively more complicated. The minigene assays indicted that the mutation c.357+1G>A resulted in an in-frame 36-amino-acid deletion in exon 6, which was consistent with a previous observation [20]. As the deletion covered the C-terminal subdomain of the paired domain, this mutation might significantly disrupt DNA binding [21]. Mutations c.-129+2T>A, c.-128–1G>C, and c.-52+1G>T in intron 2 and 3 were presumed to result in skipping of exon2 (188 bp) or exon 3 (77 bp), while exon 2 and exon 3 were located in the upstream of the coding region of *PAX6*. A previously reported mutation c.142–139T>C in intron 5–1 resulted in a significant increase in transcription of the 436 amino acid isoform (including exon 5a) and changed the ratio of isoforms 436 and 422 [22]. Mutation c.1183+5G>A in intron 12, a location that was predicted to escape the NMD process, was presumed to result in 411 amino acids of PAX6. As this mutation is located on the non-NMD region, it might cause aniridia by dominant negative mechanism. Additionally, the two missense mutations with the full-length protein, as well as a C-terminal extension mutation p.X423Lfsext*36 (the

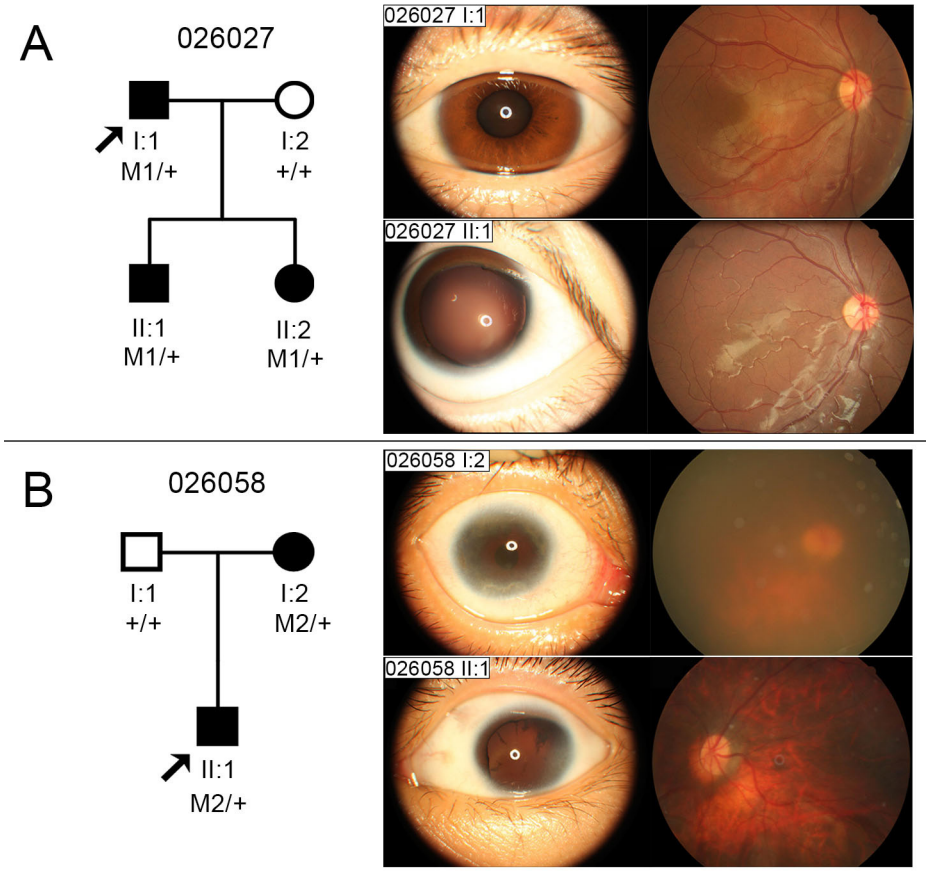

Figure 5. Pedigrees and ocular examinations of patients from families 026027 and 026058 showing intrafamilial phenotype heterogeneity. **A**: Pedigree and segregation analysis of family 026027 with mutation p.P286Lfs*79 (M1). The proband (I:1) presenting a full iris and his son (II:1) showing a partial loss of the iris. The fundus photographs of the two patients display flat foveae. **B**: Pedigree and segregation analysis of family 026058 with mutation p.N260K (M2). Anterior segment photograph of the proband (II:1) showing microcornea, partial loss of the iris, and cataract. His mother (I:2) showed aniridia-related keratopathy and a full iris. Their fundus photographs are blurred due to cataract (I:2) or showing tessellated like (II:1). + indicates wild type.

most common mutation in the current cohort), also caused aniridia by a dominant negative mechanism.

In the present cohort, we detected 11 gross deletions in 12 probands (19%, 12/63). The proportion of patients carrying large deletions (19%) was similar to that observed previously in 66 families with aniridia (15%) [11], but it was much lower than the proportion determined previously in 91 Russian families (31%) [12]. Of the 12 probands in the present study who presented with large deletions, six (50%) had a family history; this rate was much higher than the previously reported rate of about 20% [9,11,12]. All the patients with gross deletions presented typical aniridia (complete or almost complete absence of the iris), and their visual defects were no more severe than the defects found in patients with PTC mutations. Consistent with previous observations [23,24], the patients with gross deletions sparing *PAX6* had relatively mild visual defects. In this cohort, we found only three probands harboring gross deletions involving *PAX6* and *WT1*, and these patients all presented with clinical manifestations of WAGR or WAGRO syndrome. Two developed glaucoma at an early age (at 1 and 8 years old); this percentage seemed to be higher than the percentage observed in patients with gross deletions not involving *WT1*.

In this large cohort of patients with aniridia, we observed genotype–phenotype correlations to some extent. We found that about 96% (68/71) of the patients with typical aniridia carried either an intragenic mutation in *PAX6*, which would induce the NMD process, or they carried a large deletion involving *PAX6*. In contrast, the majority of patients (68%, 15/22) with partial hypoplasia of the iris or with a full iris with abnormal structure had either a run-on or missense mutation, or they had splicing mutations that did not involve the NMD process. None of the four patients with missense mutations from two unrelated families displayed typical aniridia, which was consistent with previous observations [7,10]. Six patients with mutation p.X423Lfsext*36 from four unrelated families all presented with partial hypoplasia of the iris; however, none of them had the exudative vascular retinopathy described previously in two patients with the same mutation [10]. In the present cohort, patients from five unrelated families showed intrafamilial phenotypic variability. The mutations identified in these five families included two missense, two splicing, and one frameshift deletion. As expected, the two splicing

mutations did not appear to involve the NMD process. The BCVA of the patients was usually related to patient age, ARK severity, cataract, glaucoma, foveal hypoplasia, and the choice of treatment or surgery. The five patients with gross deletion involving only *DCDC1* and *ELP4* had relative better visual acuity; however, we did not observe any other solid correlation between BCVA and the genotypes. This might be because the majority of the patients (83%) carried a gross deletion or NMD mutation, while the proportion of patients with missense mutations was small.

We did not identify any mutations in *PAX6* in two probands (patient 026071 and 026136) who presented with partial hypoplasia of the iris. These probands' disease-causing mutations might be located in the deep intronic regions of *PAX6* or in the regulatory elements downstream of *PAX6* [25,26], which were not screened, or they may reside in other genes (possibly *FOXC1*-Gene ID: 2296, OMIM: 601090, *PITX2*- Gene ID: 5308, OMIM: 601542, or *TRIM44*-Gene ID: 54765, OMIM: 612298) [9,27].

In conclusion, the present results further demonstrate that mutations in *PAX6* are the predominant cause of aniridia, and that the majority of these mutations are loss-of-function mutations that usually result in a classical aniridia phenotype. In contrast, the missense mutations, run-on mutations, and a small number of splicing mutations, which do not involve the NMD process, mostly lead to atypical aniridia and intrafamilial phenotypic variability.

APPENDIX 1. THE METHODS AND RESULTS OF STR ANALYSIS FOR HEK-293 AND ARPE-19 CELL LINE AUTHENTICATION.

To access the data, click or select the words "Appendix 1."

APPENDIX 2. PRESUMED PATHOGENIC VARIANTS IDENTIFIED IN THIS STUDY AND ANALYSIS OF THE VARIANTS BY PREDICTIVE PROGRAMS.

To access the data, click or select the words "Appendix 2."

APPENDIX 3. STHE CLINICAL FEATURES AND THE PAX6 MUTATION SCREENING RESULTS OF THE PATIENTS WITH ANIRIDIA IN THIS STUDY.

To access the data, click or select the words "Appendix 3."

APPENDIX 4. COLORED ANTERIOR SEGMENT (CAS) AND FUNDUS PHOTOGRAPHS OF PATIENTS WITH NEGATIVE *PAX6* FINDINGS.

To access the data, click or select the words "Appendix 4."

ACKNOWLEDGMENTS

This work was supported by the National Key R&D Program of China, 2016YFC0905200. The funding organization had no role in the design or conducting of this research. Financial support: This work was supported by the National Key R&D Program of China, 2016YFC0905200. The funding organization had no role in the design or conduct of this research.

REFERENCES

1. Lee H, Khan R, O'Keefe M. Aniridia: current pathology and management. Acta Ophthalmol 2008; 86:708-15. [PMID: 18937825].
2. Hingorani M, Hanson I, van Heyningen V. Aniridia. Eur J Hum Genet 2012; 20:1011-7. [PMID: 22692063].
3. Lim HT, Kim DH, Kim H. PAX6 aniridia syndrome: clinics, genetics, and therapeutics. Curr Opin Ophthalmol 2017; 28:436-47. [PMID: 28598868].
4. Ton CC, Hirvonen H, Miwa H, Weil MM, Monaghan P, Jordan T, van Heyningen V, Hastie ND, Meijers-Heijboer H, Drechsler M. Positional cloning and characterization of a paired box- and homeobox-containing gene from the aniridia region. Cell 1991; 67:1059-74. [PMID: 1684738].
5. Glaser T, Walton DS, Maas RL. Genomic structure, evolutionary conservation and aniridia mutations in the human PAX6 gene. Nat Genet 1992; 2:232-9. [PMID: 1345175].
6. Wawrocka A, Krawczynski MR. The genetics of aniridia - simple things become complicated. J Appl Genet 2018; 59:151-9. [PMID: 29460221].
7. Tzoulaki I, White IM, Hanson IM. PAX6 mutations: genotype-phenotype correlations. BMC Genet 2005; 6:27-[PMID: 15918896].
8. Wawrocka A, Sikora A, Kuszel L, Krawczynski MR. 11p13 deletions can be more frequent than the PAX6 gene point mutations in Polish patients with aniridia. J Appl Genet 2013; 54:345-51. [PMID: 23761016].
9. Ansari M, Rainger J, Hanson IM, Williamson KA, Sharkey F, Harewood L, Sandilands A, Clayton-Smith J, Dollfus H, Bitoun P, Meire F, Fantes J, Franco B, Lorenz B, Taylor DS, Stewart F, Willoughby CE, McEntagart M, Khaw PT, Clericuzio C, Van ML, Williams D, Newbury-Ecob R, Traboulsi EI, Silva ED, Madlom MM, Goudie DR, Fleck BW, Wieczorek D, Kohlhase J, McTrusty AD, Gardiner C, Yale C, Moore AT, Russell-Eggitt I, Islam L, Lees M, Beales PL, Tuft SJ, Solano JB, Splitt M, Hertz JM, Prescott TE, Shears DJ, Nischal KK, Doco-Fenzy M, Prieur F, Temple IK, Lachlan KL, Damante G, Morrison DA, van Heyningen V, FitzPatrick DR. Genetic Analysis of 'PAX6-Negative' Individuals with Aniridia or Gillespie Syndrome. PLoS One 2016; 11:e0153757-[PMID: 27124303].
10. Hingorani M, Williamson KA, Moore AT, van Heyningen V. Detailed ophthalmologic evaluation of 43 individuals with PAX6 mutations. Invest Ophthalmol Vis Sci 2009; 50:2581-90. [PMID: 19218613].

11. Bobilev AM, McDougal ME, Taylor WL, Geisert EE, Netland PA, Lauderdale JD. Assessment of PAX6 alleles in 66 families with aniridia. Clin Genet 2016; 89:669-77. [PMID: 26661695].

12. Vasilyeva TA, Voskresenskaya AA, Käsmann-Kellner B, Khlebnikova OV, Pozdeyeva NA, Bayazutdinova GM, Kutsev SI, Ginter EK, Semina EV, Marakhonov AV, Zinchenko RA. Molecular analysis of patients with aniridia in Russian Federation broadens the spectrum of PAX6 mutations. Clin Genet 2017; 92:639-44. [PMID: 28321846].

13. Souzeau E, Rudkin AK, Dubowsky A, Casson RJ, Muecke JS, Mancel E, Whiting M, Mills RA, Burdon KP, Craig JE. Molecular analysis and genotype-phenotype correlations in families with aniridia from Australasia and Southeast Asia. Mol Vis 2018; 24:261-73. [PMID: 29618921].

14. Zhang X, Tong Y, Xu W, Dong B, Yang H, Xu L, Li Y. Two novel mutations of the PAX6 gene causing different phenotype in a cohort of Chinese patients. Eye (Lond) 2011; 25:1581-9. [PMID: 21904390].

15. Zhang X, Zhang Q, Tong Y, Dai H, Zhao X, Bai F, Xu L, Li Y. Large novel deletions detected in Chinese families with aniridia: correlation between genotype and phenotype. Mol Vis 2011; 17:548-57. [PMID: 21364908].

16. Lagali N, Wowra B, Fries FN, Latta L, Moslemani K, Utheim TP, Wylegala E, Seitz B, Käsmann-Kellner B. Early phenotypic features of aniridia-associated keratopathy and association with PAX6 coding mutations. Ocul Surf 2019; [PMID: 31734509].

17. Richards S, Aziz N, Bale S, Bick D, Das S, Gastier-Foster J, Grody WW, Hegde M, Lyon E, Spector E, Voelkerding K, Rehm HL. ACMG Laboratory Quality Assurance Committee. Standards and guidelines for the interpretation of sequence variants: a joint consensus recommendation of the American College of Medical Genetics and Genomics and the Association for Molecular Pathology. Genet Med 2015; 17:405-24. [PMID: 25741868].

18. Zhang X, Wang P, Li S, Xiao X, Guo X, Zhang Q. Mutation spectrum of PAX6 in Chinese patients with aniridia. Mol Vis 2011; 17:2139-47. [PMID: 21850189].

19. Filatova AY, Vasilyeva TA, Marakhonov AV, Voskresenskaya AA, Zinchenko RA, Skoblov MY. Functional reassessment of PAX6 single nucleotide variants by in vitro splicing assay. Eur J Hum Genet 2019; 27:488-93. [PMID: 30315214].

20. Hanson IM, Seawright A, Hardman K, Hodgson S, Zaletayev D, Fekete G, van Heyningen V. PAX6 mutations in aniridia. Hum Mol Genet 1993; 2:915-20. [PMID: 8364574].

21. Mishra R, Gorlov IP, Chao LY, Singh S, Saunders GF. PAX6, paired domain influences sequence recognition by the homeodomain. J Biol Chem 2002; 277:49488-94. [PMID: 12388550].

22. Epstein JA, Glaser T, Cai J, Jepeal L, Walton DS, Maas RL. Two independent and interactive DNA-binding subdomains of the Pax6 paired domain are regulated by alternative splicing. Genes Dev 1994; 8:2022-34. [PMID: 7958875].

23. Lagali N, Wowra B, Fries FN, Latta L, Moslemani K, Utheim TP, Wylegala E, Seitz B, Käsmann-Kellner B. PAX6 Mutational Status Determines Aniridia-Associated Keratopathy Phenotype. Ophthalmology 2020; 127:273-5. [PMID: 31708273].

24. Voskresenskaya A, Pozdeyeva N, Vasilyeva T, Batkov Y, Shipunov A, Gagloev B, Zinchenko R. Clinical and morphological manifestations of aniridia-associated keratopathy on anterior segment optical coherence tomography and in vivo confocal microscopy. Ocul Surf 2017; 15:759-69. [PMID: 28698011].

25. Bhatia S, Bengani H, Fish M, Brown A, Divizia MT, de Marco R, Damante G, Grainger R, van Heyningen V, Kleinjan DA. Disruption of autoregulatory feedback by a mutation in a remote, ultraconserved PAX6 enhancer causes aniridia. Am J Hum Genet 2013; 93:1126-34. [PMID: 24290376].

26. Plaisancié J, Tarilonte M, Ramos P, Jeanton-Scaramouche C, Gaston V, Dollfus H, Aguilera D, Kaplan J, Fares-Taie L, Blanco-Kelly F, Villaverde C, Francannet C, Goldenberg A, Arroyo I, Rozet JM, Ayuso C, Chassaing N, Calvas P, Corton M. Implication of non-coding PAX6 mutations in aniridia. Hum Genet 2018; 137:831-46. [PMID: 30291432].

27. Zhang X, Qin G, Chen G, Li T, Gao L, Huang L, Zhang Y, Ouyang K, Wang Y, Pang Y, Zeng B, Yu L. Variants in TRIM44 Cause Aniridia by Impairing PAX6 Expression. Hum Mutat 2015; 36:1164-7. [PMID: 26394807].

Articles are provided courtesy of Emory University and the Zhongshan Ophthalmic Center, Sun Yat-sen University, P.R. China. The print version of this article was created on 26 March 2020. This reflects all typographical corrections and errata to the article through that date. Details of any changes may be found in the online version of the article.